Genes & Diseases (2023) 10, 1702–1713

Available online at www.sciencedirect.com

ScienceDirect

journal homepage: www.keaipublishing.com/en/journals/genes-diseases

FULL LENGTH ARTICLE

PD-L1 expression is regulated by ATP-binding of the ERBB3 pseudokinase domain

Yamu Li [a,b], Zhonghua Liu [c], Yiqing Zhao [a,b], Jie Yang [c,d,1], Tsan Sam Xiao [c], Ronald A. Conlon [a,b], Zhenghe Wang [a,b,*]

[a] *Department of Genetics and Genome Sciences, Case Western Reserve University, Cleveland, OH 44106, USA*
[b] *Case Comprehensive Cancer Center, Case Western Reserve University, Cleveland, OH 44106, USA*
[c] *Department of Pathology, Case Western Reserve University, Cleveland, OH 44106, USA*
[d] *Department of Physiology and Biophysics, Case Western Reserve University, Cleveland, OH 44106, USA*

Received 4 October 2022; received in revised form 2 November 2022; accepted 5 November 2022
Available online 8 December 2022

KEYWORDS
Colon cancer;
ERBB3;
Immunotherapy;
PD-L1;
Pseudokinase

Abstract How PD-L1 expression is regulated in cancer is poorly understood. Here, we report that the ATP-binding activity of ERBB3 pseudokinase regulates PD-L1 gene expression in colorectal cancers (CRCs). ERBB3 is one of the four members of the EGF receptor family, all with protein tyrosine kinase domains. ERBB3 is a pseudokinase with a high binding affinity to ATP. We showed that ERBB3 ATP-binding inactivation mutant reduces tumorigenicity in genetically engineered mouse models and impairs xenograft tumor growth of CRC cell lines. The ERBB3 ATP-binding mutant cells dramatically reduce IFN-γ-induced PD-L1 expression. Mechanistically, ERBB3 regulates IFN-γ-induced PD-L1 expression through the IRS1-PI3K-PDK1-RSK-CREB signaling axis. CREB is the transcription factor that regulates PD-L1 gene expression in CRC cells. Knockin of a tumor-derived ERBB3 mutation located in the kinase domain sensitizes mouse colon cancers to anti-PD1 antibody therapy, suggesting that ERBB3 mutations could be predictive biomarkers for tumors amenable to immune checkpoint therapy.

* Corresponding author. Department of Genetics and Genome Sciences, Case Western Reserve University, 10900 Euclid Avenue, Cleveland, OH 44106, USA.
E-mail address: zxw22@case.edu (Z. Wang).
Peer review under responsibility of Chongqing Medical University.
[1] Current address: Department of Integrative Structural and Computational Biology, The Scripps Research Institute, 10550 North Torrey Pines Rd, TRY-21, La Jolla, CA 92037, USA.

https://doi.org/10.1016/j.gendis.2022.11.003

Introduction

ERBB3/HER3 is a member of the EGF receptor protein tyrosine kinase family, which includes EGFR/ERBB1/HER1, ERBB2/HER2, ERBB3/HER3, and ERBB4/HER4.[1,2] Recent large-scale genomic sequencing identified ERBB3 mutations in colon,[3] gastric,[3] gallbladder,[4] and cervical cancers.[5] The EGFR family proteins have similar domain structures, including extracellular ligand-binding, transmembrane, and intracellular protein tyrosine kinase domains.[6] However, unlike the other family members, the ERBB3 kinase domain has a mutation in the HRD catalytic motif and is thus thought to be a pseudokinase with no or very low tyrosine kinase activity.[7] However, Shi and colleagues found that the pseudokinase domain of ERBB3 has a high binding affinity to ATP.[8] The lysine residue 740 (K740) in the Val-Ala-Ile-Lys (VAIK) motif in the pseudokinase domain interacts with the a and b phosphates of ATP, anchors, and orients the ATP. They showed that the ERBB3 K740M mutant abrogated its binding to ATP. Here, we report that the ATP-binding activity of ERBB3 plays a critical role in colorectal tumorigenesis.

The immune checkpoint inhibitors have revolutionized cancer therapy.[9] Tumors can suppress immune responses through increased expression of PD-L1, which binds to PD1 on cytotoxic T cells, inhibiting their function.[9] Therapeutic antibodies against PD1, PD-L1, or CTLA4, which are categorically called immune checkpoint inhibitors, have been approved by the FDA to treat a variety of human cancers.[9] However, only a fraction of cancer patients respond to immune checkpoint inhibitors. High levels of PD-L1 expression in tumors are correlated with immune checkpoint therapy in lung cancers.[10] Here we show that ERBB3 mutant colorectal cancers (CRCs) express a higher level of PD-L1 than ERBB3 WT CRCs. It is well-documented that PD-L1 expression is up-regulated by IFN-γ through the JAK-STAT signaling axis. We demonstrate here that IFN-γ induces PD-L1 expression in CRCs through the ERBB3-IRS-PI3K-PDK1-RSK-CREB signaling axis. ERBB3 E928G mutation is the most frequent recurrent mutation located in the pseudokinase domain (COSMIC database), which has been shown to be oncogenic.[3] We demonstrate here that knockin of the ERBB3 E928G oncogenic mutation into mouse colon cancer cell lines sensitizes them to anti-PD1 antibody treatment, suggesting that Erbb3 mutation could be a predictive biomarker for the identification of patients who respond to immune checkpoint inhibitors.

Materials and methods

Key resources are listed in Table S1. All animal experiments were performed in accordance with protocols approved by the IACUC committee at Case Western Reserve University.

Generation of Erbb3$^{+/K740M}$ mutant mice

Fertilized eggs from the C57Bl/6J X SJL/J F1 mice were injected with a mixture of Cas9 protein, sgRNA, and a 100 bp single-stranded DNA oligo. The repair oligo was designed to mutate lysine 740 to methionine, and destroy the PAM sequence with a synonymous mutation (Fig. 1). The K740M mutation deletes the MseI site, which was used to genotype founder animals. The knockin allele was confirmed by Sanger sequencing. Correctly targeted founder animals were genotyped using the Jackson Laboratory SNP genome scanning. A founder mouse with two alleles of C57Bl/6J chromosome 10, where the Erbb3 gene is located, was backcrossed with C57Bl/6J mice for two generations. The Erbb3$^{+/K740M}$ mice were then crossed to generate Erbb3$^{+/+}$, Erbb3$^{+/K740M}$, and Erbb3$^{K740M\ /K740M}$ littermates for the experiments.

AOM plus DSS treatment

The AOM-DSS treatment was performed as described previously.[11] Eight-week-old mice received a single intraperitoneal injection of 10 mg/kg body weight of azoxymethane (AOM) (Sigma—Aldrich, St Louis, MO, USA). One week later, the mice were treated with 2% dextran sulfate sodium (DSS Salt Reagent Grade MW 36,000—50,000, MP Biomedicals, USA) in drinking water for 7 days, followed by 10 days of usual drinking water. This DSS cycle was repeated twice. The animals were sacrificed after 53 days. Colons were removed, rinsed with PBS to remove fecal matter, sliced open longitudinally, and analyzed for the presence of tumors. Colons were fixed in 10% formalin overnight to perform histological staining after paraffin embedding.

Cdx2p-CreER^{T2} Apc$^{loxp/loxp}$ model

The Cdx2P-CreER^{T2} APC$^{loxp/loxp}$ model was described previously.[12] Two-to-three-month-old mice with the following genotypes Cdx2P-CreER^{T2} APC$^{loxp/loxp}$ Erbb3$^{+/+}$, Cdx2P-CreER^{T2} APC$^{loxp/loxp}$ Erbb3$^{+/\ K740M}$, and Cdx2P-CreER^{T2} APC$^{loxp/loxp}$ Erbb3$^{K740M/\ K740M}$ were injected intraperitoneally with 100 mg/kg body weight of tamoxifen (Sigma—Aldrich) dissolved in corn oil (Sigma—Aldrich) per day for three consecutive days. The mice were sacrificed 42 days after the tamoxifen injection, and the tumor number was counted.

Tissue culture

Human colorectal cancer cell lines DLD1, HCT116, LOVO, HT29, SW480, RKO, and genetically engineered CRC cell lines were cultured in McCoy's 5A medium with 10% fetal bovine serum (FBS). Mouse colon cancer cell line CT26 was cultured in RPMI-1640 plus 10% of FBS. MC38 cells and

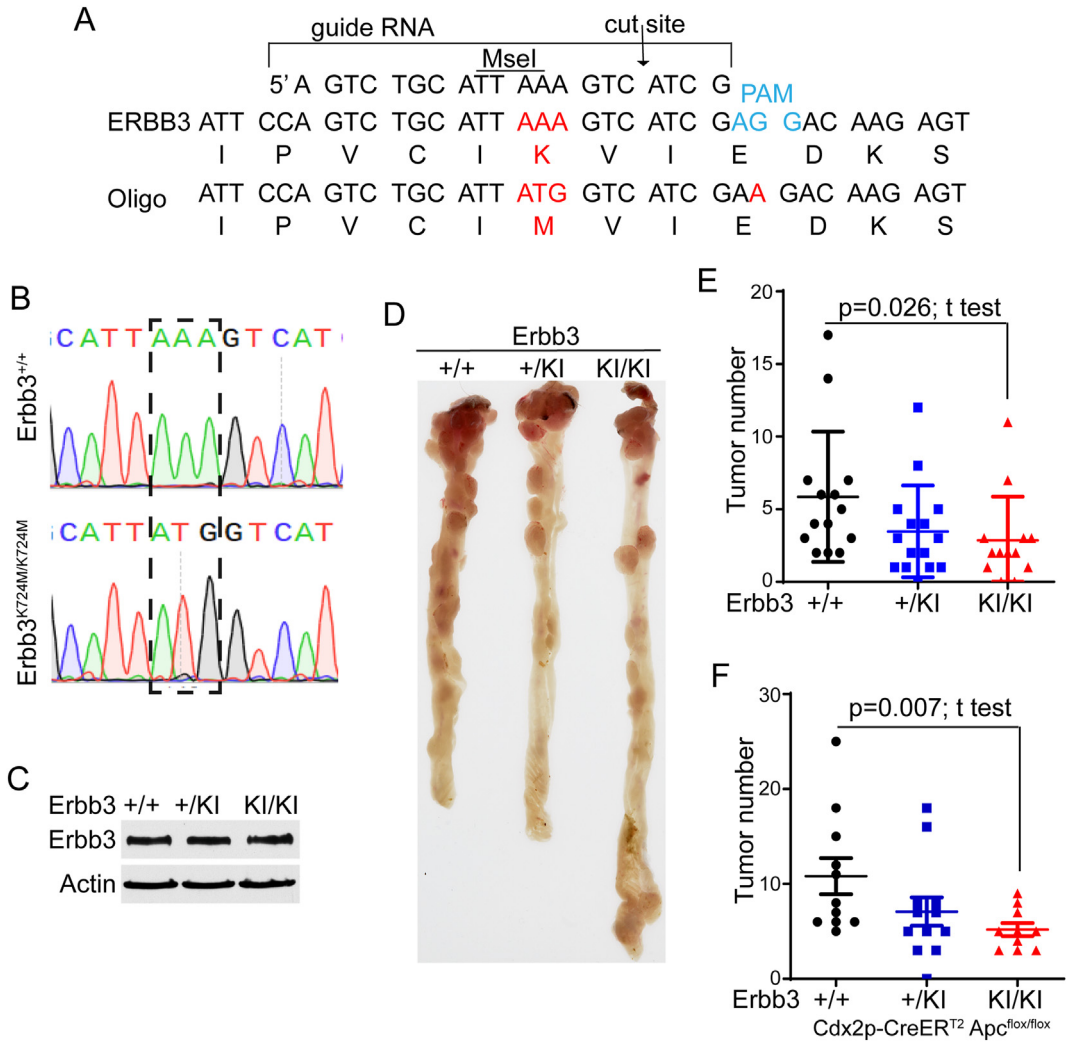

Figure 1 ERBB3 ATP-binding mutant reduces tumor growth. **(A)** Generation of ERBB3 K740M mutant knockin mice using CRISPR/Cas 9-mediated recombination. Schematic of the strategy used to generate Erbb3 K740M mutant mice. The ATP-binding lysine (K) residue was mutated to methionine (highlighted in red). The targeting oligo was designed to change the MseI restriction site for genotyping mice and a synonymous mutation to destroy the PAM sequence (highlighted in blue). Arrow indicates the Cas9 cutting site. **(B)** Genomic DNA of Erbb3$^{+/+}$ and Erbb3$^{K740M/K740M}$ mice were sequenced to confirm the generation of the desired mutation. **(C–E)** Erbb3$^{K740M/K740M}$ mutant knockin (KI) mice have reduced tumor numbers in the AOM-DSS-induced colon tumor model. Colon lysates from Erbb3$^{+/+}$ and Erbb3$^{K740M/K740M}$ littermates were blotted with the indicated antibodies **(C)**. Littermate mice of Erbb3$^{+/+}$ ($n = 14$), Erbb3$^{+/K742M}$ ($n = 15$), and Erbb3$^{K740M/K740M}$ ($n = 13$) genotypes were treated with AOM and DSS. The gross morphology of the colons from mice of the indicated genotypes is shown in **(D)**, and the number of tumors developed in each mouse is shown in **(E)**. **(F)** Erbb3$^{K740M/K740M}$ mutant mice have reduced tumor numbers in the Cdx2p-CreER^{T2}.

human embryonic kidney HEK293 cells were maintained in DMEM with 10% FBS. Mammalian cells were transfected with lipofectamine 3000 according to the manufacturer's instructions (Invitrogen). Cell proliferation was assayed using the Cell Counting Kit-8, which quantifies the number of viable cells (Dojindo Molecular Technologies, Rockville, MD). The tissue culture cell lines are routinely checked for mycoplasma contamination.

Plasmid construction

The cDNA of ERBB3 was purchased from Addgene. The full-length ERBB3 was inserted into PCMV-3Tag1A using EcoR V and Sal I restriction enzyme. Primers used in this study are listed in Table S2.

Gene targeting of cell lines

Targeting vectors were constructed with the USER system, and targeted cells were generated as described previously.[13] Briefly, homologous arms were PCR-amplified from human genomic DNA using HiFi Taq (Invitrogen) and inserted into the ZV37 vector. The mutations were introduced by site-directed mutagenesis and validated by sequencing. The gRNA constructs were made by inserting the DNA sequences encoding gRNA into the px330 vector. The gRNA

construct and the targeting vector were transfected into the target cells using lipofectamine 3000. G418-resistant clones were selected for PCR screening. Targeted clones were genotyped by PCR and sequencing. Primers for targeting vector construction and PCR screening are listed in Table S3.

Colony and focus formation in soft agar

The colony formation was described previously.[14] Briefly, cell lines were plated into 6-well plates at 400 cells per well. Cells were grown for 14 days before staining with crystal violet (Sigma, St. Louis, MO). For the soft agar assay, cell lines were plated at 5,000 cells/mL in top plugs consisting of 0.4% SeaPlaque agarose (FMC Bioproducts, Rockland, ME) and McCoy's 5A medium. After 30 days, the colonies were photographed and counted.

Xenografts

For DLD1 and LOVO cells, two million cells were injected subcutaneously and bilaterally into the flanks of 4-to-6-week-old female athymic nude mice as described.[15] Tumor volume was measured with electronic calipers, and volumes were calculated as length $\times$ width^2/2.

For CT26 and MC38 cells, 2×10^5 of WT or E928G mutant cells were injected into the flanks of 6-week-old C57BL/6 or BALB/c female mice (Jackson Lab, ME). Tumor sizes were measured every three days by caliper after implantation, and tumor volume was calculated as length $\times$ width^2 $\times$ 0.5. On day 7 after tumor cells were injected, animals were pooled and randomly divided into two groups with comparable average tumor sizes. Mice were grouped for control antibody treatment, PD-1 mAb treatment, and antibody treatments. Each treatment was administered through intraperitoneal injection (200 μg/mouse in 200 μL PBS) every three days for a total of 8 injections.

Immunoblotting

Cells were lysed in buffer containing 50 mM Tris pH 7.4, 150 mM NaCl, 5 mM EDTA, 0.5% NP40, 1 mM PMSF, and the complete protease inhibitor cocktail (Roche), supplemented with phosphatase inhibitors (1 mM Na_3VO_4, 10 mM NaF, 0.1 mM β-glycerophosphate, 20 mM sodium pyrophosphate). Equal amounts of protein were resolved by SDS-PAGE and immunoblotted with indicated antibodies. For global phospho-Ser/Thr/Tyr analyses, cells were lysed in 2 $\times$ SDS loading buffer containing 200 mM DTT and 4% SDS, 1 mM Na_3VO_4, 20 mM NaF, 0.1 mM β-glycerophosphate, and 20 mM sodium pyrophosphate. Lysates were sonicated for 5—10 s and then centrifuged at 14,000 rpm for 10 min.

Chromatin immunoprecipitation

Chromatin immunoprecipitation was performed as described previously.[16] Ten million DLD1 cells were treated with 100 ng/mL IFN-γ overnight and then cross-linked with 1% formaldehyde for 10 min at room temperature, followed by glycine termination. Cells were lysed in 0.5 mL nuclear lysis buffer (50 mM Tris—HCl, pH8.0, 10 mM EDTA, 0.5% SDS) and subjected to sonication. Two hundred μL of the sonicated nuclear lysate was diluted in 800 μL dilution buffer (20 mM Tris—HCl, 150 mM NaCl, 2 mM EDTA, 1% Triton X-100) and incubated with normal IgG or anti-CREB antibody overnight, followed by incubating with Protein A conjugated magnetic beads for 2 h at 4°C. The samples were washed with RIPA buffer (20 mM Tris—HCl, pH8.0, 150 mM NaCl, 2 mM EDTA, 1% Triton X-100, 0.1% SDS) 8 times, washing buffer (20 mM Tris—HCl, pH 8.0, 500 mM NaCl, 2 mM EDTA, 1% Triton X-100, 0.1% SDS) twice, and TE buffer (10 mM Tris—HCl, pH 8.0, 1 mM EDTA) twice. The IP products were eluted with 200 μL elution buffer (1% SDS, 0.1 M $NaHCO_3$) followed by reverse cross-linked chromatin at 65°C overnight. After being treated with proteinase K (0.3 μg/μL) at 37°C for 2 h, DNAs were purified using the PCR purification kit (Qiagen). Purified DNA was used for quantitative PCR analyses and was normalized to 1% input chromatin.

Real-time PCR

Cultured cells were disrupted in lysis buffer from the RNeasy Mini Kit (Qiagen), and total RNA was purified following the manufacturer's instructions. cDNA was synthesized using the Transcriptor First Strand cDNA Synthesis Kit (Roche). Then iTaqTM Universal SYBR® Green Supermix (Bio-rad) was employed to perform quantitative PCR on a CFX ConnectTM Real-Time PCR Detection System (Bio-rad). Gene expressions were determined using the $2^{-\Delta\Delta Ct}$ method, normalizing to housekeeping genes Actin. The primers used were listed in Table S3.

RNA interference

Interfering RNAs (siRNA) targeting JAK1, JAK2, IRS1, PDK1, RSK1, RSK2, RSK3, CREB, and its appropriate non-silencing control were synthesized by Integrated DNA Technologies IDT. The siRNAs were transfected into cells using Lipofectamine 3000 with siRNA (10 nmol/L final concentration) in Opti-MEM. After 48 h, cells were treated with 100 ng/mL IFN-γ before harvest.

Luciferase reporter assay

The human PDL1 promoter fragment was amplified from the genomic DNA of DLD1 cells using Pfu polymerase (Agilent) and cloned into a pGL3-Basic luciferase reporter vector and confirmed by sequencing. Luciferase reporter assays were performed in DLD1, and LOVO cells using the Dual-Luciferase Reporter Assay System (Promega) according to the manufacturer's instructions. Luciferase activity was measured using the GloMax-Multi Microplate Reader (Promega).

Quantification and statistical analysis

GraphPad Prism software was used to create the graphs. Data are plotted as mean $\pm$ standard error of the mean. We applied the *t*-test to compare the means between the two groups, assuming unequal variances. For xenograft growth, we carried out ANOVA for repeated measurements to test

whether there was an overall difference in the tumor sizes by testing group differences, as well as whether there was a difference in the development of tumor sizes over time between the two groups by testing the interaction between time and group.

Results

ERBB3 kinase inactivation reduces tumorigenicity in mice

Given that the ERBB3 pseudokinase has a high binding affinity to ATP and that ERBB3 is mutated in CRCs,[3,8] we set out to interrogate the role of the pseudokinase domain in colorectal tumorigenesis. To this end, we generated ERBB3 K740M, which was reported to reduce its ATP binding ability,[8] mutant KI mice using CRISPR/Cas9 genome editing (Fig. 1A, B). While ERBB3 null mice are recessive embryonic lethal,[17,18] Erbb3$^{K740M/K740M}$ mice are viable and fertile with no obvious developmental defects. The K740M mutation did not affect ERBB3 protein levels in the colons of mice (Fig. 1C). We then treated Erbb3$^{WT/WT}$, Erbb3$^{WT/K740M}$ Erbb3$^{K740M/K740M}$ littermate mice with AOM and DSS. As shown in Figure 1D, E, and S1A, Erbb3$^{K740M/K740M}$ mice developed significantly fewer colon tumors compared to the WT mice.

We next examine how the Erbb3 kinase-inactivating mutant impacts colon tumorigenesis in a carcinogen-independent model. To this end, we crossed Erbb3$^{WT/K740M}$ mice into the Cdx2p-CreER^{T2} Apc$^{flox/flox}$ genetic background, and tumors were induced by conditional inactivation of the Apc gene in the colon through a Cdx2p-driven Cre transgene. As shown in Figure 1F and S1B, Erbb3$^{K740M/K740M}$ mice form significantly fewer tumors than Erbb3$^{WT/WT}$ mice. Notably, Erbb3$^{WT/K740M}$ heterozygous mice also showed a trend of reduced tumor numbers (Fig. 1E, F). Taken together, the data suggest that the ATP-binding activity of ERBB3 plays an oncogenic role in colon tumorigenesis.

ERBB3 K742M ATP-binding mutation impairs the tumorigenicity of human colorectal cancer cells

To determine if the ERBB3 ATP-binding site mutant impacts the tumorigenicity of human CRCs, we knocked in (KI) the K742M (equivalent to mouse K740M) mutation in CRC cell lines using CRISPR/Cas9 genome editing. We chose DLD1 and LOVO cell lines because they express relatively high levels of ERBB3 (Fig. S2A). Of 76 G418-resistant DLD1 clones and 100 LOVO clones, 3 homozygous KI clones were identified in DLD1 and 2 in LOVO (Fig. 2A). We chose two clones from each of the two cell lines for in-depth characterization. As shown in Figure S2B, the K742M mutation did not affect the levels of ERBB3 protein. To ensure that the observed phenotypes of the KI clones are due to the mutated pseudokinase domain, we reconstituted the KI clones with Flag-tagged wild-type ERBB3 (Fig. 2B, C).

Compared to their parental cells, ERBB3 K742M mutant KI clones derived from both DLD1 and LOVO grew slower in tissue culture (Fig. S2C, D) and formed fewer colonies in a colony-forming assay (Fig. S2E, F). Moreover, the mutant cell clones formed fewer soft-agar foci compared to the parental cells (Fig. S2G, H), whereas the reconstitution of WT ERBB3 largely restored the deficiency in anchorage-independent growth (Fig. S2G, H). Interestingly, compared to the parental cells, the DLD1 ERBB3 KI clones grew significantly slower as xenograft tumors (Fig. 2D, E), whereas the LOVO ERBB3 KI clones failed to form xenograft tumors (Fig. 2F, G). Nonetheless, the WT ERBB3 reconstituted cells largely rescued these defects (Fig. 2D—G). Together, these data suggest that the ERBB3 pseudokinase promotes colorectal tumorigenesis.

ERBB3 ATP-binding mutant CRCs impair IFN-γ-induced PD-L1 expression

It has been reported recently that overexpression of ERBB3 tumor-derived mutations in gallbladder cancer cells resulted in the up-regulation of PD-L1 RNA expression.[19] We thus mined the TCGA colorectal adenocarcinoma dataset (Pan-Cancer Atlas) to determine if CRCs harboring ERBB3 mutations express higher levels of PD-L1. As shown in Figure 3A, ERBB3 mutant CRCs express significantly higher levels of PD-L1 than ERBB3 WT CRCs.

We next set out to determine if the ERBB3 ATP-binding activity modulates PD-L1 expression. Given that interferon-γ (IFN-γ) is a major cytokine that stimulates PD-L1 expression in cancer cells, we treated DLD1 and LOVO ERBB3 kinase-inactivating mutant (K742M) KI clones and their corresponding parental (WT) cells with or without IFN-γ. As shown in Figure 3B and C, IFN-γ induced PD-L1 protein expression in both DLD1 and LOVO parental cells. However, the induction of PD-L1 by IFN-γ was much reduced in the DLD1 and LOVO K742M KI clones (Fig. 3B, C). Reconstitution of WT ERBB3 restores IFN-γ induced PD-L1 protein expression (Fig. S3A). Moreover, IFN-γ induced over 30-fold PD-L1 mRNA expression in both DLD1 and LOVO parental cells (Fig. 3D, E), whereas the induction of PD-L1 gene expression was greatly reduced in the ERBB3 kinase-inactivating mutant KI clones (Fig. 3D, E). Together, these data demonstrate that the ERBB3 pseudokinase modulates IFN-γ-mediated signaling pathway(s) that activates PD-L1 gene expression.

ERBB3 kinase regulates PD-L1 expression through the IRS1-PI3K-PDK1-RSK signaling axis

It is well documented that IFN-γ induces PD-L1 expression through the STAT signaling pathways,[20] we thus examined if the ERBB3 K742M mutant impacted the phosphorylation of the STAT proteins. As shown in Figure S3B, the ERBB3 K742M ATP-binding mutant did not affect IFN-γ-activated STAT1, STAT3, and STAT5 phosphorylation in DLD1 cells, whereas the other STAT proteins are not expressed in colon cancer cells. Moreover, the ERBB3 K742M mutant did not affect IFN-γ-induced Erk activation (Fig. S3B).

Given that ERBB3 binds to IRS1,[21] we examined IRS1 knockout DLD1 cells[15] and found IRS1 knockout attenuated IFN-γ-induced PD-L1 expression (Fig. 3F). Consistently, IRS1 knockdown in LOVO cells also reduced IFN-γ-induced PD-L1 expression (Fig. S3C). Because PI3K is downstream of IRS1, we next examined whether inhibition of PI3K reduced IFN-γ-induced PD-L1 expression. As shown in Figure S3D and E,

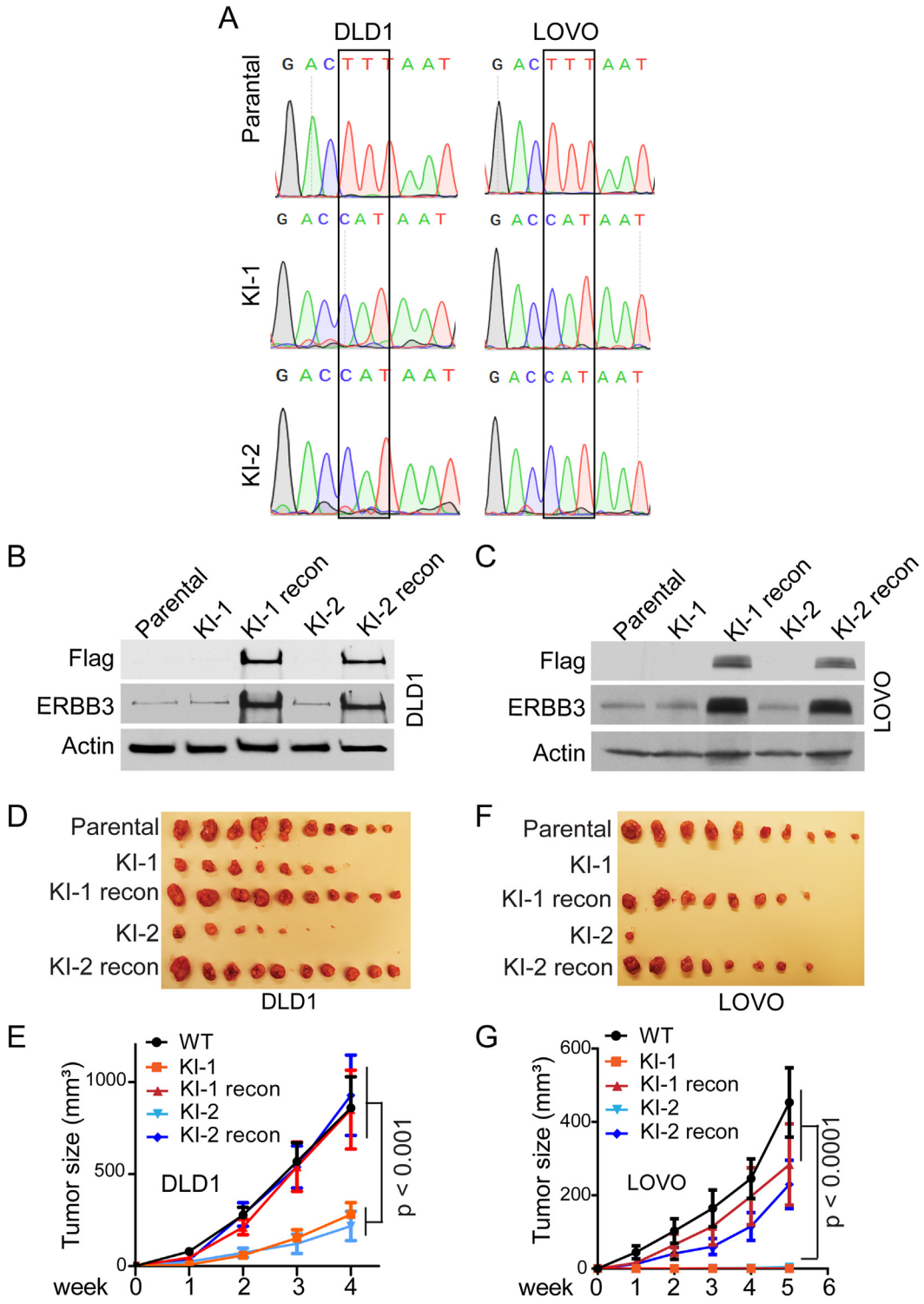

Figure 2 ERBB3 ATP-binding mutant human CRCs reduce tumorigenicity in xenograft models. **(A)** Generation of ERBB3 K742M mutant knockin (KI) clones. DLD1 and LOVO CRC cell lines were targeted with CRISPR/Cas 9-mediated recombination. The parental cells and homozygous KI clones were sequenced to confirm the generation of the desired mutation. KI-1 and KI-2 are two independently-derived homozygous KI clones. **(B, C)** The ERBB3 K742M mutation does not affect ERBB3 protein expression. Cell lysates from the indicated cell lines were blotted with antibodies against either ERBB3 or Actin. **(D—G)** The indicated cells were injected subcutaneously and bilaterally into nude mice (5/group). Tumor sizes were measured weekly and the tumors were then harvested (D, E). The growth curves of the tumors are shown in (F). ANOVA was used for the statistical analyses. KI: ERBB3 K742M mutant knockin; KI recon: the KI clone reconstituted with WT ERBB3.

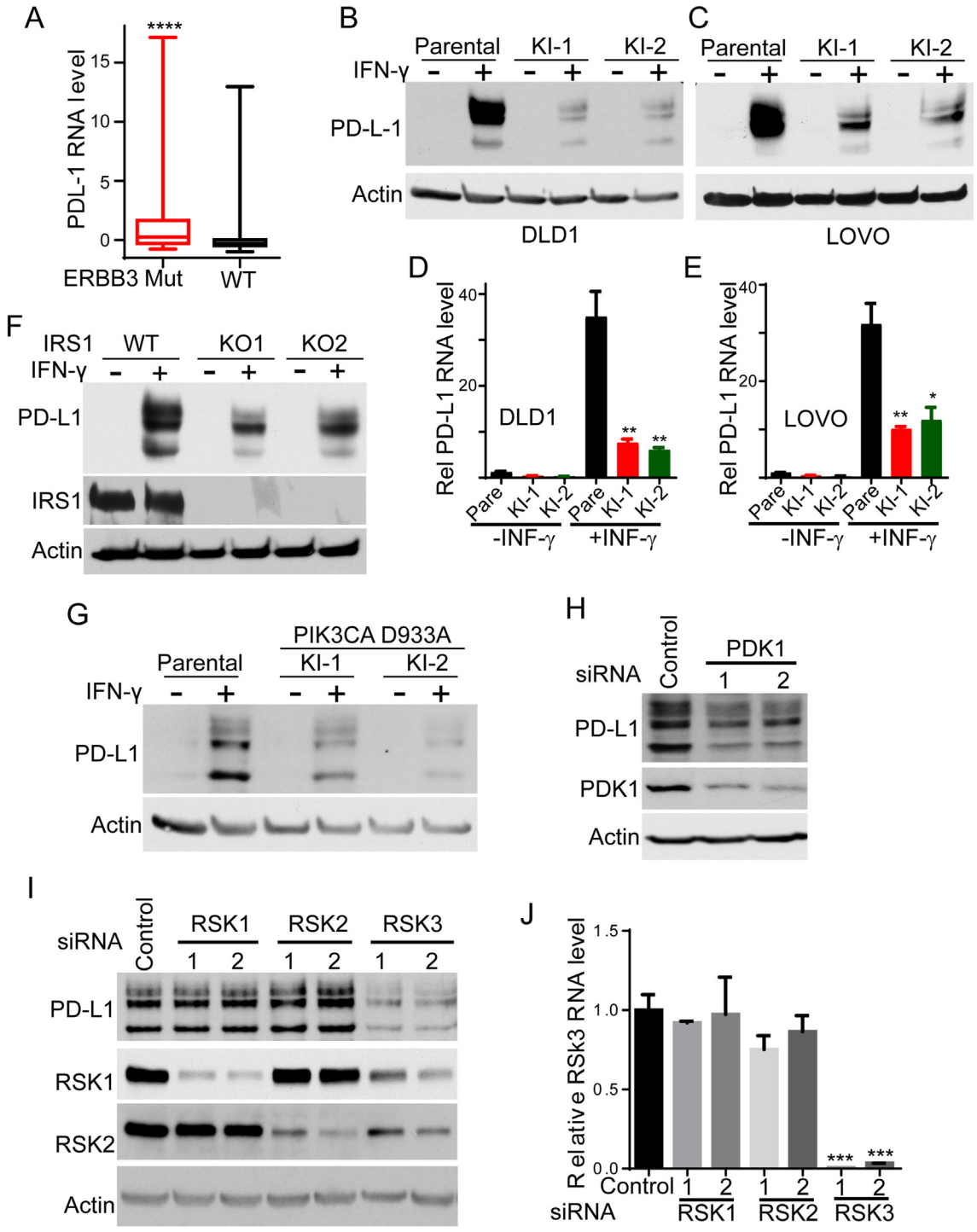

Figure 3 ERBB3-IRS1-PI3K-PDK1-RSK signaling axis regulates IFN-γ-induced PD-L1 expression. **(A)** Erbb3 mutant colorectal cancers (CRCs) express higher levels of PD-L1. The expression levels of PD-L1 (RNA-seq data in the TCGA PanCancer Atlas dataset) are plotted into Erbb3 mutant ($n = 29$) and WT ($n = 503$) colorectal cancer groups. ****$P < 0.0001$, Mann—Whitney test. **(B—E).** The Erbb3 kinase modulates PD-L1 gene expression. The indicated Erbb3 K742M mutant KI and their corresponding parental (WT) cells were treated with or without IFN-γ for 24 h. Cell lysates were blotted with the indicated antibodies (B, C). PD-L1 mRNA levels were measured by q-RT-PCR (D, E). *$P < 0.05$, **$P < 0.01$, *t*-test. **(F)** IRS1 knockout attenuates IFN-γ-induced PD-L1 expression. DLD1 parental or IRS1 knockout clones were treated with or without IFN-γ. Cell lysates were blotted with the indicated antibodies. **(G)** p110α kinase-inactivating mutant attenuates IFN-γ-induced PD-L1 expression. DLD1 parental cells and PIK3CA/p110α mutant clones were treated with or without IFN-γ. Cell lysates were blotted with the indicated antibodies. **(H)** PDK1 knockdown reduces IFN-γ-induced PD-L1 expression. DLD1 cells were transfected with control or two independent siRNA against PDK1 and then treated with IFN-γ. Cell lysates were blotted with the indicated antibodies. **(I, J)** RSK knockdown reduces IFN-γ-induced PD-L1 expression. DLD1 cells were transfected with the indicated siRNAs and then treated with IFN-γ. Cell lysates were blotted with the indicated antibodies. RSK3 knockdown was measured by qRT-PCR because of a lack of specific antibodies. ***$P < 0.0001$, *t*-test.

both p110α inhibitor BYL-719 and GDC0326 suppressed IFN-γ-induced PD-L1 expression in DLD and LOVO CRC cells in a dose-dependent manner. Consistently, p110α kinase-inactivating mutant DLD1 cells that we generated previously[14] also attenuated IFN-γ-induced PD-L1 expression (Fig. 3G). Similarly, PDK1 inhibitor BX795 suppressed IFN-γ-induced PD-L1 expression in DLD and LOVO CRC cells in a dose-dependent manner (Fig. S3F). These results were further validated by two independent siRNAs against PDK1 (Fig. 3H; Fig. S3G).

Given that AKT is downstream of IRS-PI3K-PDK1 signaling, we were surprised that the ERBB3 ATP-binding mutant did not impact IFN-γ-induced AKT phosphorylation (Fig. S3B). Because we and others have shown that RSK activity is also regulated by the PI3K-PDK1 pathway,[14,22] we tested if the ERBB3 kinase-inactivating mutant affects RSK activation. As shown in Figure S3B, compared to parental DLD1 cells, IFN-γ-induced RSK phosphorylation is attenuated in the Erbb3 K742M kinase-inactivating mutant KI clones. To test if RSK regulates PD-L1 expression, we treated DLD1 and LOVO CRC cells with a pan-RSK inhibitor BI-D1870. As shown in Figure S3H, BI-D1870 inhibited IFN-γ-induced PD-L1 expression in a dose-dependent manner. RSK has four different isoforms: RSK1, RSK2, RSK3, and RSK4. But RSK4 is not expressed in DLD1 and LOVO cells. We then tested if the knockdown of each of them impacted PD-L1 expression. As shown in Figure 3I, J and S3I, the knockdown of either RSK1 or RSK2 did not affect IFN-γ-induced PD-L1 expression in DLD1 and LOVO cells. However, the knockdown of RSK3 with two independent siRNA, which also downregulated RSK1 and RSK2 protein levels (Fig. 3I, J; Fig. S3I), markedly reduced IFN-γ-induced PD-L1 expression in DLD1 and LOVO cells (Fig. 3I; Fig. S3I). Together, these data suggest that the ERBB3-IRS1-PI3K-PDK-RSK pathway regulates IFN-γ-induced PD-L1 expression in CRCs.

The transcription factor CREB regulates PD-L1 expression

To identify the transcription factor(s) that mediates the induction of PD-L1 expression by the aforementioned signaling axis, we examined transcription factors that were known to be regulated by RSK. As shown in Figure 4A, CREB

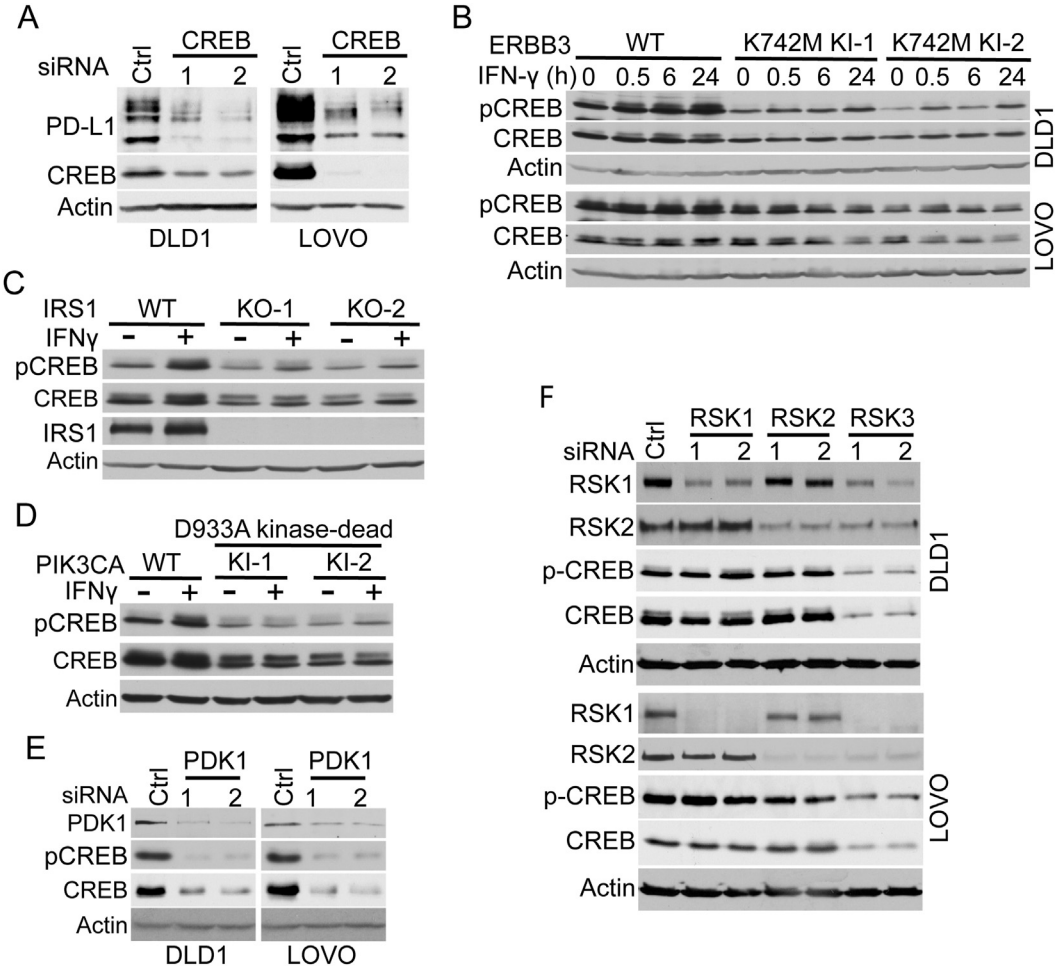

Figure 4 ERBB3-IRS1-PI3K-PDK1-RSK-CREB signaling axis regulates IFN-γ-induced PD-L1 expression. **(A)** CREB knockdown reduces IFN-γ-induced PD-L1 expression. **(B)** IFN-γ-induced CREB phosphorylation and CREB protein levels are reduced in ERBB3 kinase-dead mutant cells. **(C)** IFN-γ-induced CREB phosphorylation and CREB protein levels are reduced in IRS1 knockout cells. **(D)** IFN-γ-induced CREB phosphorylation and CREB protein levels are reduced in PIK3CA/p110α kinase-dead mutant cells. **(E)** PDK1 knockdown reduces IFN-γ-induced CREB phosphorylation and CREB protein levels. **(F)** Knockdown of RSKs reduces IFN-γ-induced CREB phosphorylation and CREB protein levels.

knockdown drastically reduced IFN-γ-induced PD-L1 expression in both DLD1 and LOVO cells, whereas knockdown of ATF4, CEBPβ, or p65 did not reduce IFN-γ-induced PD-L1 expression (Fig. S4A, B). We next examined if the ERBB3-IRS-PI3K-PDK1-RSK signaling axis modulates CREB. ERBB3 ATP-binding mutant cells reduced CREB protein levels and attenuated IFN-γ-induced CREB phosphorylation (Fig. 4B), and so did the IRS1 knockout clones p110α kinase-inactivating mutant KI clones (Fig. 4C, D). Moreover, the knockdown of PDK1 or RSKs reduced CREB protein levels and attenuated IFN-γ-induced CREB phosphorylation (Fig. 4E, F). These results suggest that the ERBB3-IRS-PI3K-PDK1-RSK signaling axis transduces the signal from IFN-γ to stabilize and activate CREB-mediated PD-L1 expression.

To determine if CREB binds to the PD-L1 promoter and directly activates PD-L1 gene expression, we searched the PD-L1 promoter region and found four putative CREB binding sites (Fig. 5A). Our chromatin immunoprecipitation analyses showed that CREB bound to the first three sites within a 1 KB promoter region of PD-L1 (Fig. 5B). We thus cloned the 1 KB promoter region into a luciferase reporter to measure CREB-driven PD-L1 gene expression. As shown in Figure 5C, overexpression of CREB increased the reporter activity, whereas its knockdown in LOVO cells reduced the PD-L1 reporter activity (Fig. 5D). We then transfected the reporter into DLD1 and LOVO parental and ERBB3 kinase-inactivating mutant cells. As shown in Figure 5E and F, IFN-γ induced high levels of luciferase activity in both DLD1 and LOVO parental cells. However, the reporter activities were attenuated in the ERBB3 kinase-inactivating mutant cells (Fig. 5E, F). Taken together, the data suggest that IFN-γ activates the ERBB3-IRS-PI3K-PDK1-RSK-CREB signaling axis to activate PD-L1 gene expression in CRC cells (Fig. 5G).

Tumor-derived ERBB3 kinase activating mutation sensitizes colon cancers to immune checkpoint therapy

Having demonstrated that the ERBB3 pseudokinase regulates PD-L1, we set out to determine if tumor-derived ERBB3 mutations located in the pseudokinase domain impact PD-L1 expression and colon cancers' response to immune checkpoint therapy. We chose to knock in the ERBB3 E928G mutation into mouse colon cancer cell lines because it is the most frequent recurrent mutation located in the pseudokinase domain (COSMIC database). We used CRISPR/Cas9 genome editing technology to knock in the E928G mutation into mouse colon cancer cell lines CT26 and MC38. At least two independently derived ERBB3 E928G knockin clones were obtained from each cell line by genomic DNA sequencing analyses (Fig. S5A). The E928G mutation did not affect its protein levels in both CT26 and MC38 cell lines (Fig. 6A, B). Nonetheless, IFN-γ induced higher levels of PD-L1 in the ERBB3 E928G mutant knockin CT26 and MC38 clones than in corresponding parental cells and an off-target clone (WT), in which ERBB3 alleles remain WT, but the cell went through the same gene targeting process (Fig. 6C, D). To test how the E928G mutant knockin cells respond to immune checkpoint therapy, we established syngeneic mouse tumor models with parental cells, off-target clones, and the ERBB3 E928G mutant knockin clones. The mice were treated with either control IgG or an anti-PD1 therapeutic antibody. The parental cells and off-target clones behaved similarly (Fig. S5B—D). For simplicity, we only show data of the off-target clone and the ERBB3 E928G mutant knockin clones in Figure 6E and F. We believe that the off-target clones are better controls because any unexpected immune responses caused by the CRISPR/Cas9 gene targeting would be manifested in the off-target clones. Interestingly, the anti-PD1 therapeutic antibody exerted greater tumor inhibition in the ERBB3 E928G mutant knockin clones than in the off-target clones (Fig. 6E, F). Notably, PD-L1 levels were increased in ERBB3 E928G mutant knockin tumors (Fig. S5E). Together, the data provide compelling evidence supporting the notion that tumor-derived ERBB3 mutation located in the pseudokinase domain sensitizes colon cancer to immune checkpoint inhibitors.

Discussion

Our studies uncover a previously unrecognized signaling pathway that regulates IFN-γ-induced PD-L1 gene expression. Although it is well-documented that IFN-γ induces PD-L1 gene expression through the JAK-STAT signaling,[20,23] our data demonstrate that the ERBB3-IRS1-PI3K-PDK1-RSK-CREB signaling axis also regulates IFN-γ induces PD-L1 expression. Our data are consistent with a previous study showing that PTEN loss leads to the up-regulation of PD-L1 in glioma.[24] Li et al recently reported that overexpression of ERBB3 results in the up-regulation of PD-L1 expression,[19] suggesting that ERBB3 transduces the signal to regulate PD-L1. However, they did not identify the mechanisms by which ERBB3 modulates PD-L1 gene expression. We provide here compelling evidence that the ERBB3 pseudokinase transduces the signal through the IRS1-PI3K-PDK1-RSK pathway and activates CREB-mediated PD-L1 gene expression. It is worth noting that EGFR regulates PD-L1 levels through posttranslational modifications,[25,26] which is distinct from the mechanisms we identify in this study. We find that CREB is the transcription factor activated by this signaling axis that modulates PD-L1 gene expression. However, our data do not exclude the possibility that STAT proteins can cooperate with CREB to activate IFN-γ to induce PD-L1 gene expression. Given that PD-L1 modulates tumor growth by immune evasion, it is possible that the reduced PD-L1 levels in ERBB3 K740M mutant cells may contribute to its slow growth *in vivo*.

Our studies suggest that ERBB3 mutation may sensitize cancer to immune checkpoint inhibitor therapy. The FDA approved anti-PD1 antibody pembrolizumab for the treatment of metastatic MSI-high colorectal cancer patients, which account for ~4% of metastatic colorectal cancer.[27] Although most microsatellite-stable (MSS) CRCs do not respond to immune checkpoint inhibitors, many clinical trials indicate that a small fraction of MSS CRCs does respond to immune checkpoint inhibitors.[27] Therefore, there is an

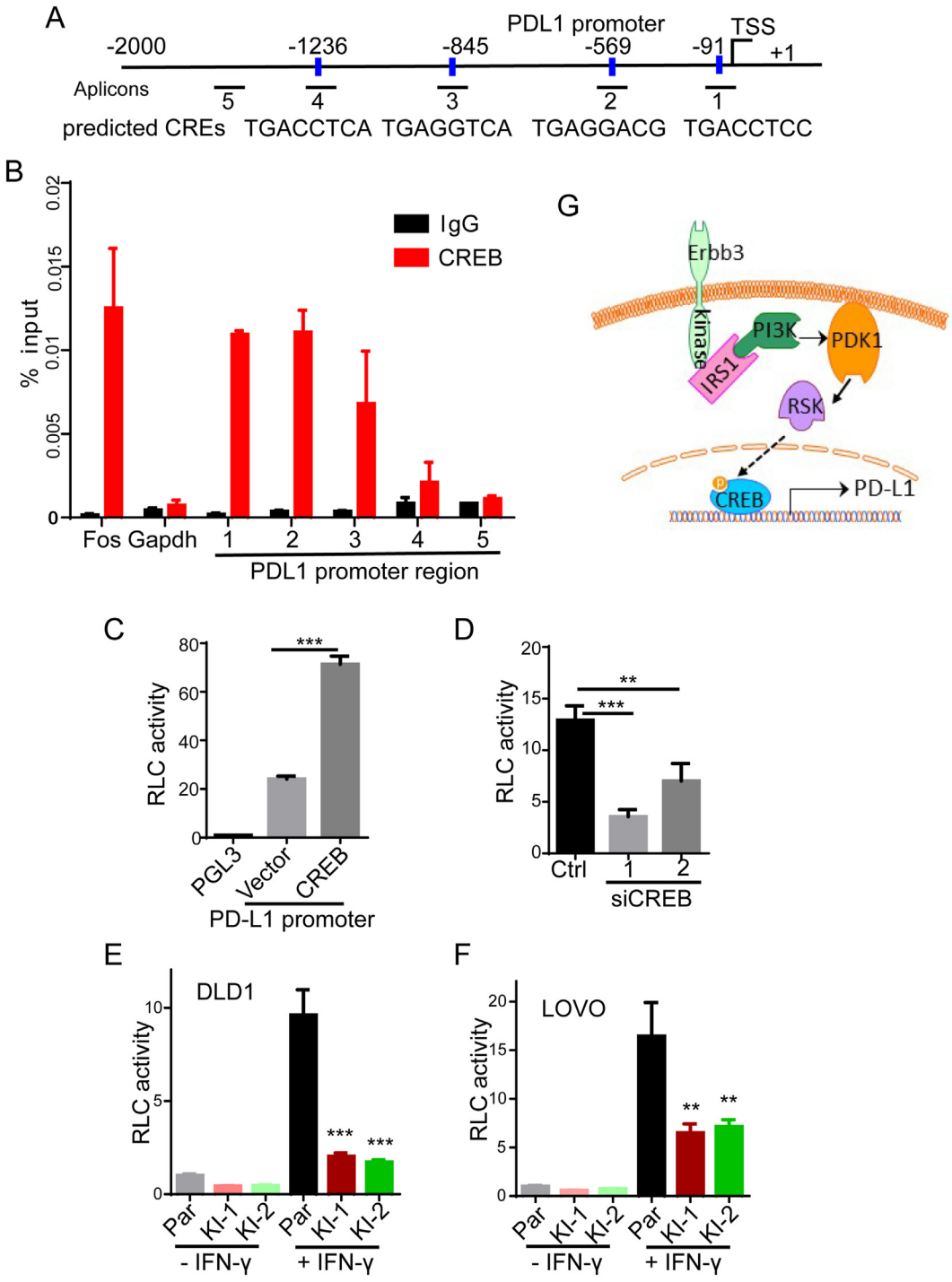

Figure 5 CREB regulates PD-L1 gene expression. **(A)** Schematics of predicted CREB binding sites in the PD-L1 promoter region. **(B)** ChIP-qPCRs show that CREB binds to the first 3 CREB binding sites. **(C)** Overexpression of CREB increases PD-L1 transcriptional activity. **(D)** CREB knockdown reduces PD-L1 transcriptional activity. **(E, F)** ERBB3 kinase-inactivating mutant reduces IFN-γ-induced PD-L1transcriptional activity. A luciferase reporter of the PDL1 promoter containing three CREB binding sites was transfected into the indicated cell lines. Cells were treated with or without IFN-γ and harvested for luciferase assay. $^{**}P < 0.01$, $^{***}P < 0.001$, *t*-test. **(G)** A model of IFN-γ induces PD-L1 expression through the ERBB3-IRS1-PI3K-PDK1-RSK-CREB signaling axis.

urgent need for additional biomarkers that identify microsatellite-stable CRCs, which should respond to checkpoint inhibitors. Our data demonstrate that knockin of oncogenic ERBB3 E928G into two different mouse colon cancer cell lines sensitizes them to anti-PD1 antibody treatment, suggesting that ERBB3 mutation may sensitize human colorectal

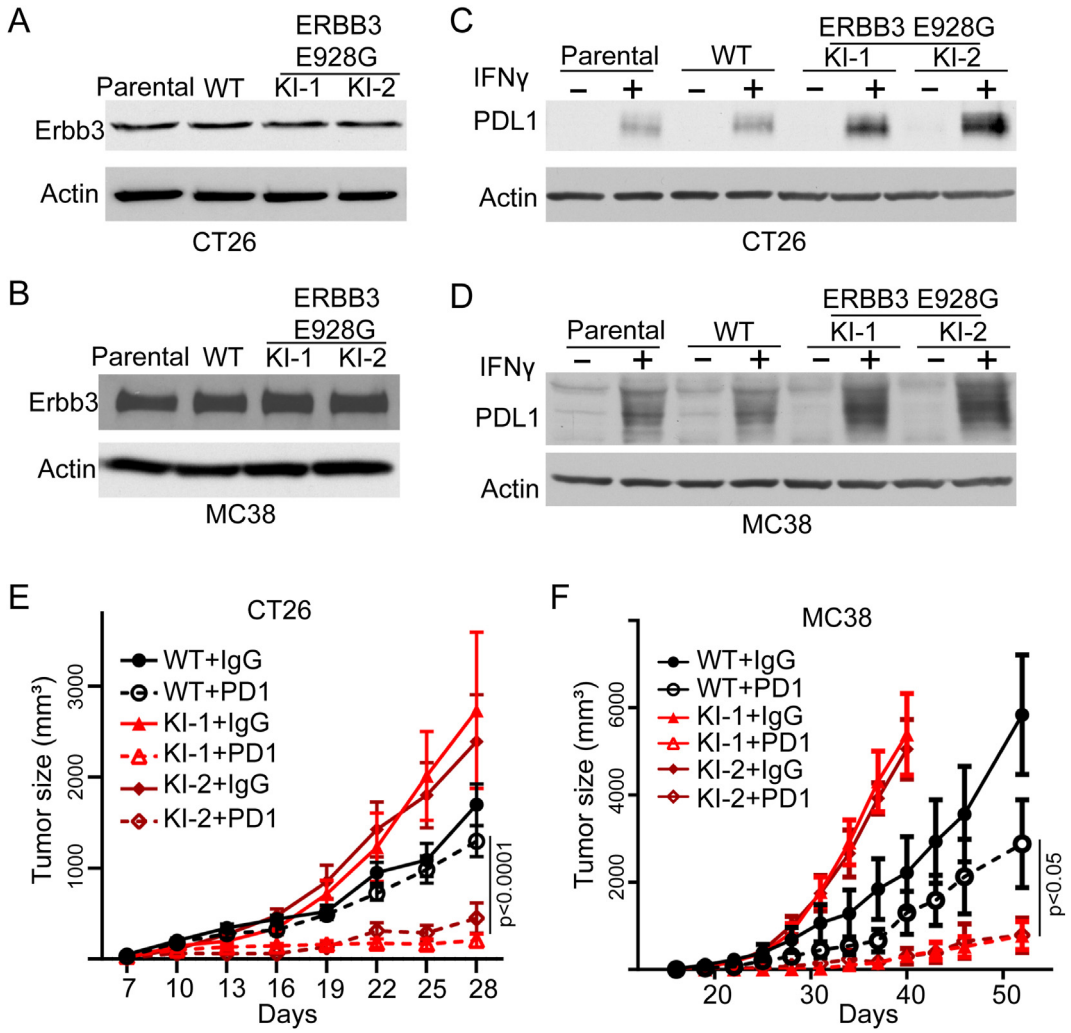

Figure 6 A tumor-derived ERBB3 mutation located in the pseudokinase domain sensitizes mouse colon cancer to an anti-PD1 therapeutic antibody. **(A, B)** ERBB3 E928G mutation does not impact its protein levels. Cell lysates of CT26 or MC38 parental independently-derived E928G mutant knockin clones were blotted with the indicated antibodies. **(C, D)** The Erbb3 E928G mutation increases IFN-γ-induced PD-L1 expression. CT26 or MC38 parental off-target clone (WT) E928G KI cells were treated with or without IFN-γ. Cell lysates were blotted with the indicated antibodies. **(E, F)** The Erbb3 E928G mutation sensitizes CT26 mouse colon cancer to an anti-PD1 therapeutic antibody. CT26 or MC38 off-target clone (WT) and two independently-derived E928G KI clones were injected subcutaneously into syngeneic mice. The mice were treated with 8 doses of control IgG or an anti-PD1 (200 μg) therapeutic antibody every other day starting on day 7 after injection of the cells (10 mice/group). ANOVA was used for statistical analysis.

cancer patients to immune checkpoint inhibitors as well. Although PD-L1 expression levels are correlated with clinical response to anti-PD1 antibody treatment in lung cancer patients,[28] the correlation between PD-L1 level and response to an anti-PD1 antibody in CRCs is yet to be established. The mechanisms by which the ERBB3 E928G oncogenic mutation sensitizes CRCs to anti-PD1 antibody treatment warrant further studies.

Author contributions

Funding acquisition: ZW; Conceptualization: ZW and YL; Experimental design: ZW, YL, RAC, and TSX; Experiment implementation: YL, ZL, YZ, Data analyses: YL, JY, SX, and ZW; Manuscript writing: ZW, RAC, and YL.

Conflict of interests

The authors declare no conflict of interests.

Funding

This work was supported by the National Institutes of Health (NIH) grants (No. R01CA256791, R01CA264320, P50CA150964, and P30CA043703).

Acknowledgements

We thank Dr. Cathy Carlin for her critical reading of this manuscript.

Appendix A. Supplementary data

Supplementary data to this article can be found online at https://doi.org/10.1016/j.gendis.2022.11.003.

References

1. Kraus MH, Fedi P, Starks V, et al. Demonstration of ligand-dependent signaling by the erbB-3 tyrosine kinase and its constitutive activation in human breast tumor cells. *Proc Natl Acad Sci U S A*. 1993;90(7):2900—2904.
2. Arteaga CL, Engelman JA. ERBB receptors: from oncogene discovery to basic science to mechanism-based cancer therapeutics. *Cancer Cell*. 2014;25(3):282—303.
3. Jaiswal BS, Kljavin NM, Stawiski EW, et al. Oncogenic *ERBB3* mutations in human cancers. *Cancer Cell*. 2013;23(5):603—617.
4. Li M, Zhang Z, Li X, et al. Whole-exome and targeted gene sequencing of gallbladder carcinoma identifies recurrent mutations in the ErbB pathway. *Nat Genet*. 2014;46(8):872—876.
5. Cancer Genome Atlas Research Network, Albert Einstein College of Medicine. Analytical Biological Services, et al. Integrated genomic and molecular characterization of cervical cancer. *Nature*. 2017;543(7645):378—384.
6. Lemmon MA, Schlessinger J. Cell signaling by receptor tyrosine kinases. *Cell*. 2010;141(7):1117—1134.
7. Guy PM, Platko JV, Cantley LC, et al. Insect cell-expressed p180erbB3 possesses an impaired tyrosine kinase activity. *Proc Natl Acad Sci U S A*. 1994;91(17):8132—8136.
8. Shi F, Telesco SE, Liu Y, et al. ErbB3/HER3 intracellular domain is competent to bind ATP and catalyze autophosphorylation. *Proc Natl Acad Sci U S A*. 2010;107(17):7692—7697.
9. Wei SC, Duffy CR, Allison JP. Fundamental mechanisms of immune checkpoint blockade therapy. *Cancer Discov*. 2018;8(9):1069—1086.
10. Topalian SL, Hodi FS, Brahmer JR, et al. Safety, activity, and immune correlates of anti-PD-1 antibody in cancer. *N Engl J Med*. 2012;366(26):2443—2454.
11. Zhao Y, Zhang X, Guda K, et al. Identification and functional characterization of paxillin as a target of protein tyrosine phosphatase receptor T. *Proc Natl Acad Sci U S A*. 2010;107(6):2592—2597.
12. Zhao Y, Zhao X, Chen V, et al. Colorectal cancers utilize glutamine as an anaplerotic substrate of the TCA cycle *in vivo*. *Sci Rep*. 2019;9(1):19180.
13. Zhang X, Guo C, Chen Y, et al. Epitope tagging of endogenous proteins for genome-wide ChIP-chip studies. *Nat Methods*. 2008;5(2):163—165.
14. Hao Y, Samuels Y, Li Q, et al. Oncogenic PIK3CA mutations reprogram glutamine metabolism in colorectal cancer. *Nat Commun*. 2016;7:11971.
15. Hao Y, Wang C, Cao B, et al. Gain of interaction with IRS1 by p110α-helical domain mutants is crucial for their oncogenic functions. *Cancer Cell*. 2013;23(5):583—593.
16. Hao Y, He B, Wu L, et al. Nuclear translocation of p85β promotes tumorigenesis of PIK3CA helical domain mutant cancer. *Nat Commun*. 2022;13(1):1974.
17. Riethmacher D, Sonnenberg-Riethmacher E, Brinkmann V, et al. Severe neuropathies in mice with targeted mutations in the ErbB3 receptor. *Nature*. 1997;389(6652):725—730.
18. Erickson SL, O'Shea KS, Ghaboosi N, et al. ErbB3 is required for normal cerebellar and cardiac development: a comparison with ErbB2-and heregulin-deficient mice. *Development*. 1997;124(24):4999—5011.
19. Li M, Liu F, Zhang F, et al. Genomic *ERBB2*/*ERBB3* mutations promote PD-L1-mediated immune escape in gallbladder cancer: a whole-exome sequencing analysis. *Gut*. 2019;68(6):1024—1033.
20. Prestipino A, Zeiser R. Clinical implications of tumor-intrinsic mechanisms regulating PD-L1. *Sci Transl Med*. 2019;11(478):eaav4810.
21. Knowlden JM, Gee JM, Barrow D, et al. erbB3 recruitment of insulin receptor substrate 1 modulates insulin-like growth factor receptor signalling in oestrogen receptor-positive breast cancer cell lines. *Breast Cancer Res*. 2011;13(5):R93.
22. Anjum R, Blenis J. The RSK family of kinases: emerging roles in cellular signalling. *Nat Rev Mol Cell Biol*. 2008;9(10):747—758.
23. Cha JH, Chan LC, Li CW, et al. Mechanisms controlling PD-L1 expression in cancer. *Mol Cell*. 2019;76(3):359—370.
24. Parsa AT, Waldron JS, Panner A, et al. Loss of tumor suppressor PTEN function increases B7-H1 expression and immunoresistance in glioma. *Nat Med*. 2007;13(1):84—88.
25. Akbay EA, Koyama S, Carretero J, et al. Activation of the PD-1 pathway contributes to immune escape in EGFR-driven lung tumors. *Cancer Discov*. 2013;3(12):1355—1363.
26. Li CW, Lim SO, Chung EM, et al. Eradication of triple-negative breast cancer cells by targeting glycosylated PD-L1. *Cancer Cell*. 2018;33(2):187—201.
27. Ganesh K, Stadler ZK, Cercek A, et al. Immunotherapy in colorectal cancer: rationale, challenges and potential. *Nat Rev Gastroenterol Hepatol*. 2019;16(6):361—375.
28. Bodor JN, Boumber Y, Borghaei H. Biomarkers for immune checkpoint inhibition in non-small cell lung cancer (NSCLC). *Cancer*. 2020;126(2):260—270.